Cement and Concrete Research 41 (2011) 923–931

Contents lists available at ScienceDirect

Cement and Concrete Research

journal homepage: http://ees.elsevier.com/CEMCON/default.asp

Compatibility studies between N-A-S-H and C-A-S-H gels. Study in the ternary diagram Na_2O–CaO–Al_2O_3–SiO_2–H_2O

I. Garcia-Lodeiro [a,b,*], A. Palomo [b], A. Fernández-Jiménez [b], D.E. Macphee [a,**]

[a] Department of Chemistry, University of Aberdeen, Meston Walk, Old Aberdeen, AB24 3UE, UK
[b] Eduardo Torroja Institute (C.S.I.C), Serrano Galvache 4, 28033, Madrid, Spain

ARTICLE INFO

Article history:
Received 21 July 2010
Accepted 17 May 2011

Keywords:
CSH (B)
TEM (B)
Stability (C)
Alkali Activated Cement (D)
N-A-S-H

ABSTRACT

Sodium aluminosilicate hydrate (N-A-S-H) gel, the main reaction product of the alkali-activated aluminosilicates, differs of the aluminium-modified calcium silicate hydrate (C-A-S-H) gel of PC pastes. Increasing the level of SCM to reduce PC content of binders are being considered to address reduction in CO_2 emissions, activation of the additional SCM content by alkali activation represents a possible environmentally sustainable solution. Therefore, mixtures of C-A-S-H and N-A-S-H gels might be anticipated and the present study assesses the compatibility relationships between them.

Compositional diagrams are provided to indicate phase compositional ranges and the phase assemblages obtained under equilibrium conditions. In calcium-rich formulations (pH in excess of 12), C-A-S-H and C_2ASH_8 form as stable phases. However, in the lime poor part of the diagram an amorphous gel (N,C)-A-S-H precipitates but its stability is dependent on system pH and available Ca. (N,C)-A-S-H gels are de-stabilised by Ca to give C-A-S-H gels in suitable systems.

Contents

1. Introduction

In the context of addressing environmental issues, specifically reducing CO_2 emissions, the possibility of diluting Portland cement with high volumes of SCMs (Supplementary Cementitious Materials) is currently being considered. However, by diluting the PC (Portland cement) content, the ability to activate the SCM is reduced and the use of additional alkaline activator offers a possible solution.

The study of alkali activation of aluminosilicates is a relatively new field when compared with traditional Portland cement-containing systems [1–4]. Alkali-activated aluminosilicates are differentiated from hydrated Portland cements by their higher initial alkalinity and the absence of lime. This is already sufficient to define quite different hydration products from the different systems so that predictions of

* Correspondence to: I. Garcia-Lodeiro, Eduardo Torroja Institute (C.S.I.C), Serrano Galvache 4, 28033, Madrid, Spain. Tel: +34 91 302 04 40; fax: +34 91 302 6047.
** Corresponding author.
E-mail addresses: iglodeiro@ietcc.csic.es (I. Garcia-Lodeiro), d.e.macphee@abdn.ac.uk (D.E. Macphee).

0008-8846/$ – see front matter © 2011 Elsevier Ltd. All rights reserved.
doi:10.1016/j.cemconres.2011.05.006

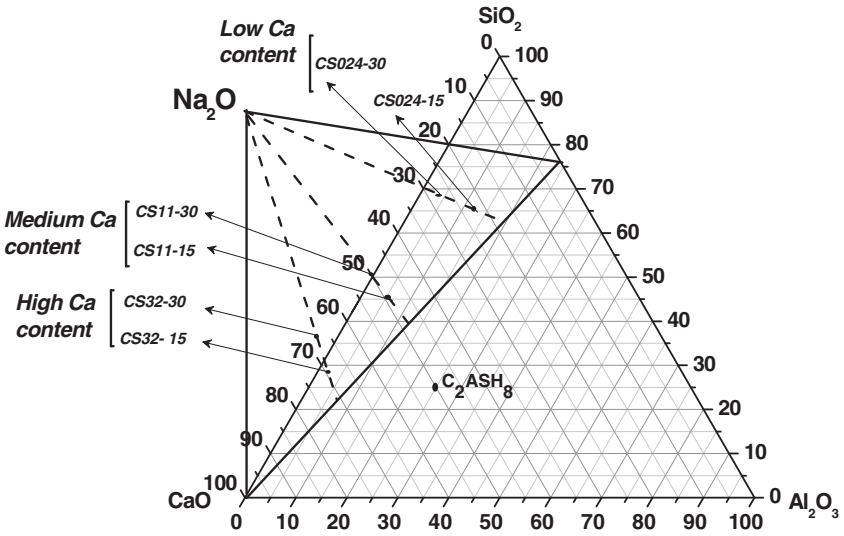

Fig. 1. Modified $CaO–Al_2O_3–SiO_2$ compositional diagram to indicate bulk compositions of mixtures used in the precipitation/solubility study. Compositions lie above the $CaO–Al_2O_3–SiO_2$ plane towards the projected Na_2O apex. All phases are water saturated.

the properties of alkali-activated aluminosilicates made based on Portland cement chemistry are inappropriate. Whereas the main binding phase of hydrated Portland cement is an aluminate-substituted calcium silicate hydrate (C-(A)-S-H) gel, the main product in alkali activated systems is sodium aluminosilicate hydrate gel designated N-A-S-H.

The compatibility of the two cementitious gels (C-(A)-S-H and N-A-S-H) has important implications for hybrid Portland cement – alkali activated aluminosilicate systems in which both products might be expected [5–9]. Previous studies using synthetic gels explored the effects of the constituents of each gel on the other, i.e. high pH conditions and the presence of aqueous aluminate strongly influence C-S-H composition and structure [7,8] and aqueous Ca modifies N-A-S-H gels leading to a partial replacement of sodium with calcium to form (N,C)-A-S-H gels [9]. Despite these observations, the conditions required for such modifications have not been fully defined and with the possibility of constructional cements having both gels co-existing, a systematic study of N-A-S-H – C-A-S-H compatibility seems appropriate.

2. Experimental procedure

In assessing gel properties and compatibilities, two approaches have been adopted: (i) solids for characterisation have been precipitated from solutions of soluble salts (precipitation/dissolution approach), and *ii)* pre-synthesised gels have been mixed directly prior to ageing.

Table 1
Compositions (mol.%) chosen for precipitation in the ternary diagram the $Na_2O–CaO–Al_2O_3–SiO_2–H_2O$.

	NaOH mmol (% Na_2O)	$Ca(OH)_2$ mmol (% CaO)	$Al(OH)_3$ mmol (% Al_2O_3)	SiO_2 mmol (aerosil) (% SiO_2)
CS32-15	8.00 (15%)	16.00 (59.95%)	3.34 (6.26%)	5.01 (18.79%)
CS32-30	19.44 (30%)	16.00 (49.36%)	3.34 (5.16%)	5.01 (15.48%)
CS11-15	12.26 (15%)	16.00 (39.15%)	4.68 (11.46%)	14.05 (34.39%)
CS11-30	29.76 (30%)	16.00 (32.25%)	4.68 (9.43%)	14.05 (28.32%)
CS024-15	37.15 (15%)	16.00 (12.92%)	44.63 (18.02%)	66.94 (54.06%)
CS024-30	90.22 (30%)	16.00 (10.64%)	44.63 (14.84%)	66.94 (44.52%)

Labels indicate CaO/SiO_2 ratio and sodium content of initial mix composition (e.g. CS32-15 indicates an initial CaO/SiO_2 ratio of 3.2 and a Na_2O content of 15 mol.%)

2.1. Precipitation/dissolution approach

A series of 6 mixtures of aqueous solutions was prepared, comprising sodium aluminate (prepared using NaOH and $Al(OH)_3$ (Fisher)), sodium silicate (prepared using Aerosil SiO_2 (Degussa) and NaOH (BDH Convol®), and a $Ca(OH)_2$ (Sigma-Aldrich) slurry, in proportions appropriate to strategic positions within the $Na_2O–CaO–Al_2O_3–SiO_2–H_2O$ system (mol %) (see Fig. 1, Table 1). Synthesis and solubility experiments were performed under a N_2 atmosphere to minimise to the influence of atmospheric CO_2.

Experiments were conducted from both supersaturation and undersaturation approaches according to Fig. 2 and consistent with similar previous studies [7,8]. Aqueous composition data were obtained [10] and solids were characterized by different techniques (XRD, FTIR, DTA/TG and TEM/EDX) in both approaches. As we have similar results in both approaches only the undersaturation results will be reported and discussed.

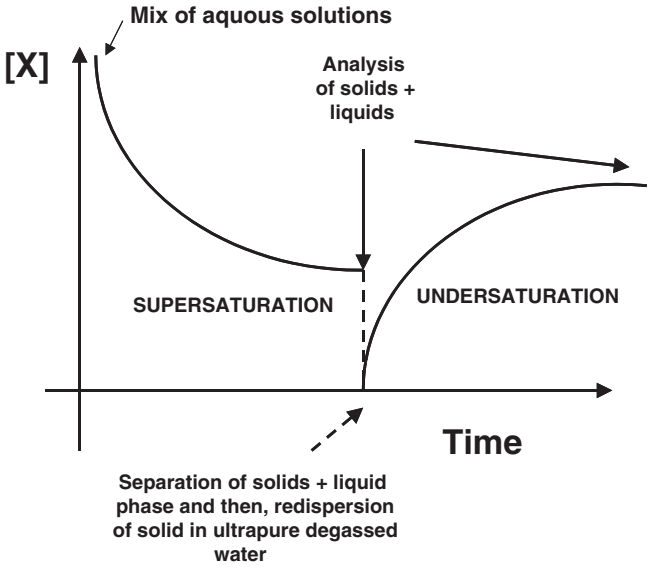

Fig. 2. Experimental design.

XRD data were obtained using a Bruker D8 Advance powder diffractometer. TG/DTA measurements were carried out using a Stanton Redcroft STA 781 thermal analyser at a heating rate of 10 °C/min.

FTIR spectra were obtained using an ATIMATTSON FTIR-TM series spectrophotometer. Specimens were prepared by mixing 1 mg of sample with 300 mg of KBr. The range of spectral analysis was 2000–400 cm^{-1}. Finally TEM characterization was conducted using a JEOL 200EX. TEM microscope fitted with a LINK AN10/855 EDX analyzer.

2.2. Direct mixing of gels

Two series of 50/50 wt.% mixtures of dried pre-formed C-S-H and N-A-S-H and C-A-S-H and N-A-S-H gels were re-dispersed in ultra pure degassed water with continuous stirring. Solid samples were taken at different ages and analysed by FTIR and TEM/EDX.

The pre-formed gels were synthesized using a previously reported precipitation procedure [7–9]. N-A-S-H gels were prepared using sodium silicate and sodium aluminate solutions, whereas C-S-H gel was synthesized using sodium silicate and saturated $Ca(OH)_2$ solutions. In the synthesis of C-A-S-H gels, sodium aluminate was used as the source of aluminium and in the preparation of the N-A-S-H the SiO_2/Al_2O_3 ratio was 2. The CaO/SiO_2 and SiO_2/Al_2O_3 ratios to prepare C-S-H were 1.2 and 0 respectively, and for C-A-S-H, they were 1.2 and 2.25 respectively. The absence of additional materials precipitated together with the control gels (N-A-S-H, C-A-S-H and C-S–H) was tested by XRD and TEM/EDX. Only a small amount of carboaluminates was detected during the analyses of the C-A-S-H gel and there was no evidence for alumina or silica gels. A small weight loss and endotherm at higher temperatures may be related to carbonate or to the dehydration of alumina or silica gels but none of these have been confirmed.

All processes, including synthesis, drying (over saturated $CaCl_2$ solution) and mixing of gels were carried out under an N_2 atmosphere to minimise carbonation of the samples. All experiments were conducted at 25 °C.

3. Results and discussion

3.1. Precipitation/dissolution approach

Fig. 3(a) and (b) shows XRD patterns from precipitates from the two extremes of bulk composition, CS32 and CS024 respectively, corresponding to the highest and lowest calcium environments during initial mixing (i.e. mix identifier indicates relevant initial $CaO:SiO_2$ ratios—see Table 1). Data for the intermediate calcium loaded sample are not shown because these results were similar to the results obtained for the high calcium-loaded (CS32) samples.

The XRD diffraction pattern for the CS32 sample shows some crystalline peaks assigned to strätlingite (gehlenite hydrate) and carboaluminates as well as some broad peaks associated with the precipitation of C-S-H gel. The results for precipitates from low calcium environments are quite different; in this case only an amorphous halo located between 20–35 2θ is observed. Despite careful avoidance strategies, including working under a N_2 atmosphere, some peaks were observed which are assigned to calcite.

The extent of carbonation was determined by DTA/TG. Results generally show a group of endotherms located in the interval between 60 and 150 °C associated to the loss of evaporable water from the gel (see for example, Fig. 4). The presence of an endotherm around 258 °C is attributed to the loss of bound water in calcium aluminosilicates [11]. However, it is significant that the endotherms typical of carbonates between 600–800 °C are absent, suggesting that carbonation takes place during XRD analyses. A small weight loss and endotherm at higher temperatures may be related to carbonate but this is not confirmed.

Fig. 5(a) and (b) shows the FTIR spectra for high and low calcium environments respectively. Typical spectra for C-A-S-H and N-A-S-H gels are included in the figure. Fig. 5(a) shows that the high calcium environment provides practically the same vibrations that are observed for a C-A-S-H gel [8,12,13]; the main band around 960 cm^{-1} associated with asymmetrical stretching vibrations of Si–O bonds (ν_{as} Si–O–Si) and the bands located at lower wavenumbers assigned to deformation vibrations (δ Si–O–Si/ δ Si–O–Al). Therefore these spectra indicate structural characteristics similar to those representative of C-A-S-H gel structures. In contrast, the low calcium environment gels show quite different results; the vibration bands are broader and asymmetrical and the main band (ν_{as} T–O: where T is Si or Al [13,14]) appears shifted towards higher wavenumbers. The position of this band is more typical of the main band in N-A-S-H gels [13,14].

Fig. 6 shows the results of TEM/EDX analyses. TEM micrographs are identified with ranges of compositions expressed as clusters of points projected on the $CaO-Al_2O_3–SiO_2$ plane of a $Na_2O–CaO–Al_2O_3–SiO_2$ phase diagram. It is to be noted that Na_2O and H_2O are also components of the relevant system; all phases are assumed to be water saturated.

High and medium calcium environments show two distinct clusters; the first group, designated 'C-A-S-H' and highlighted by the range of

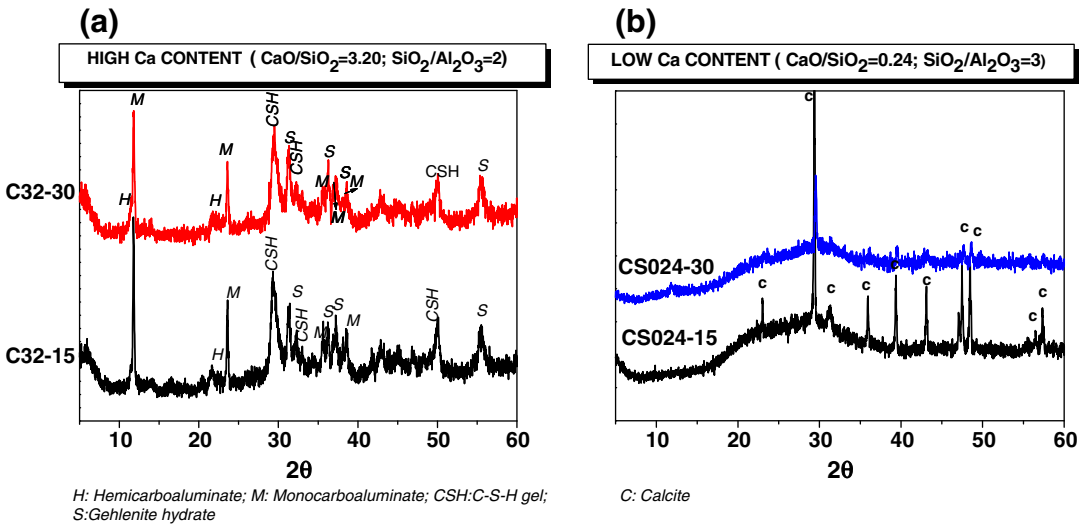

Fig. 3. XRD patterns for samples prepared with (a) high (b) low calcium environments.

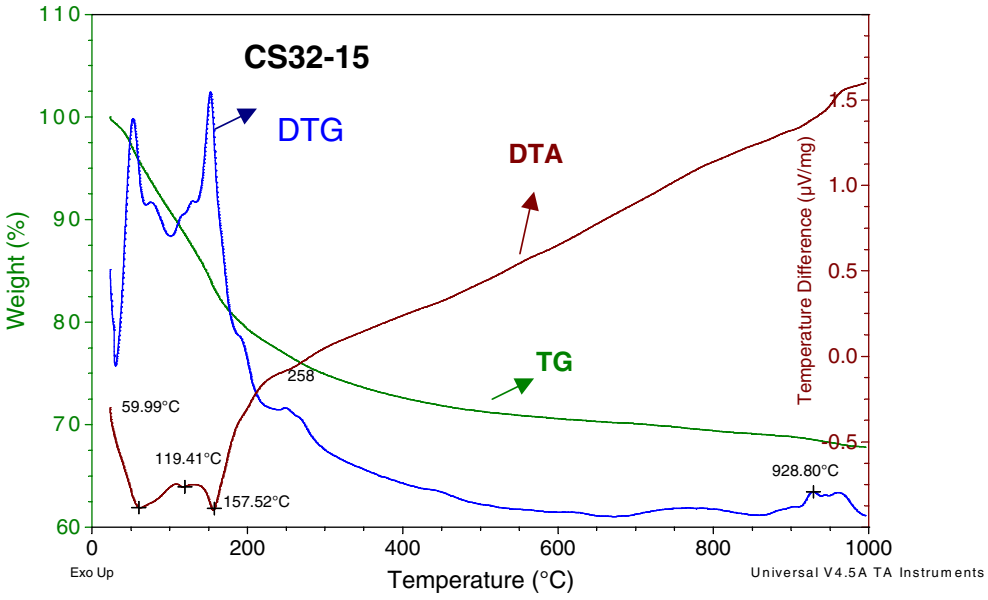

Fig. 4. DTA/TG data for sample CS32-15.

compositions within the indicated region, appeared to be single phase, C-A-S-H gels. Relevant particle morphologies are indicated alongside the various clusters and no crystalline material was observed either by morphology or by electron diffraction. The more lime-rich cluster is associated with a mixture of crystalline and amorphous phases. In this case, EDX compositions can therefore not be considered reliable indicators of gel compositions but instead are likely to represent average compositions of the different phases interacting with the electron beam. Indeed, possibilities for co-existing phases in this region include $Ca(OH)_2$, gehlenite hydrate and high lime C-A-S-H gel. Further, XRD indicates the presence of carboaluminate phases which is consistent with this region of the diagram as discussed below.

Gels derived from a low calcium environment show a separate cluster of compositions. In fact, unlike the higher calcium-bearing gels which had negligible Na_2O content and lie virtually on the $CaO–Al_2O_3–SiO_2$ plane, these compositions are elevated above the plane of the diagram and are correspondingly associated with a certain Na_2O content. This cluster, identified as calcium substituted N-A-S-H gels ((N,C)-A-S-H), is associated with only one gel having globular morphology, slightly different to the morphology shown by a C-A-S-H gel (See Fig. 6).

3.1.1. Tentative phase diagram

A representation of possible phase equilibria in the $Na_2O–CaO–Al_2O_3–SiO_2$ system at 25 °C is shown in Fig. 7. The recent study by Pardal et al.[15] confirms that the compositional range indicated by the field designated 'C-A-S-H' in Fig. 6 is too extensive to correspond to single phase C-A-S-H despite our observations of 'single phase'. However, a tentative phase diagram which remains consistent with both the literature and our own results can still be proposed based on the following indicators:

- the low CaO/SiO_2 limit observed in the present study is close to that observed by Pardal et al.[15] and this is therefore projected towards Al_2O_3 to define their reported Al saturated limit at composition $C_{0.72}A_{0.1}SH_x$.
- a reduction in the maximum Al_2O_3/SiO_2 limit with increasing CaO/SiO_2 is indicated [15] defining the edge of the C-A-S-H field to a limiting composition of $C_{0.95}A_{0.06}SH_x$.
- with further increases in CaO/SiO_2 we tentatively propose that Al_2O_3/SiO_2 remains constant to a composition of $C_{1.94}A_{0.06}SH_x$. This Ca-rich extreme is approximately consistent with the observed compositions of C-S-H in Portland cement systems.

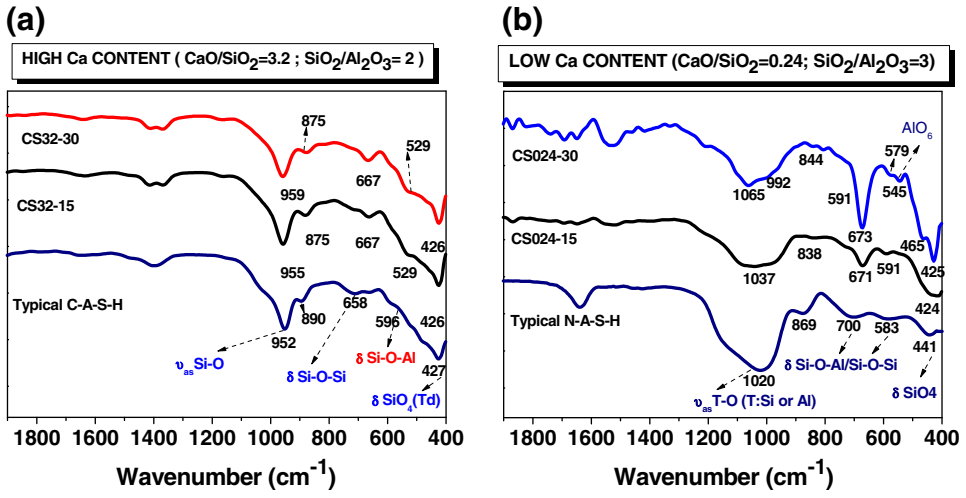

Fig. 5. FTIR samples in (a) high (b) low calcium environments.

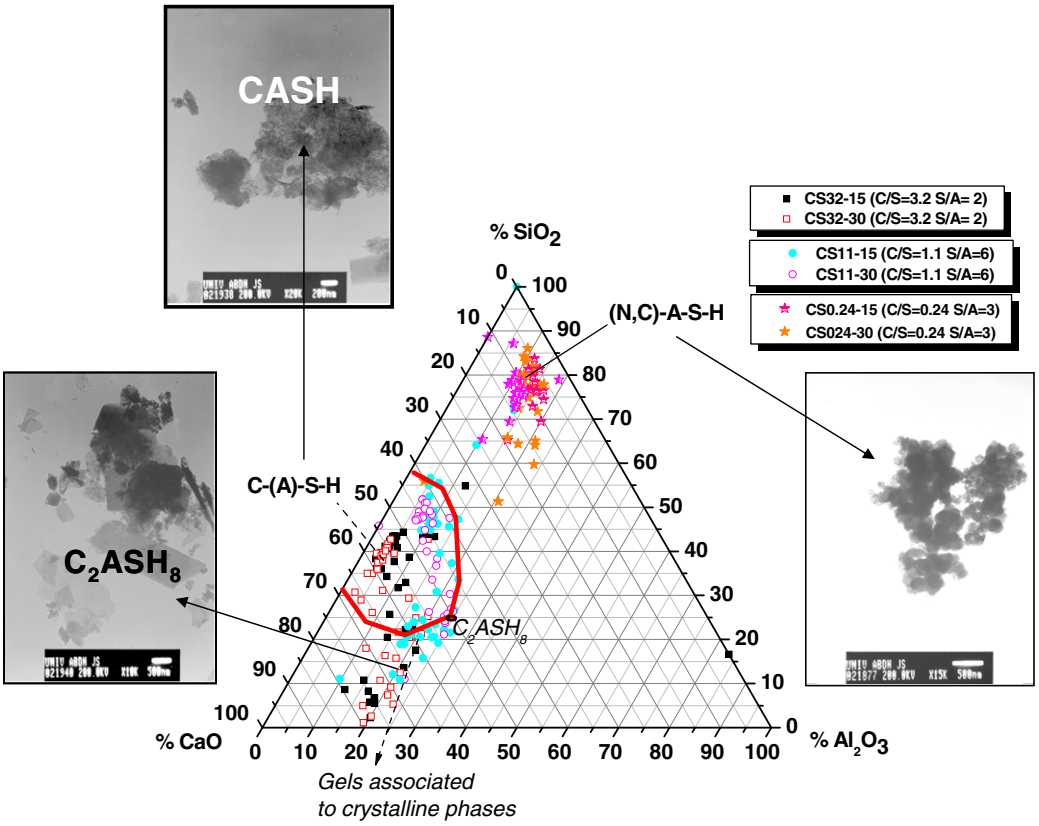

Fig. 6. EDX analyses of precipitated gels projected onto the $CaO–Al_2O_3–SiO_2$ plane of the $Na_2O–CaO–Al_2O_3–SiO_2–H_2O$ system diagram. Original bulk aqueous compositions are indicated in the figure legend by the label format $CS(CaO/SiO_2)$–(mol.% Na_2O); e.g. CS32-15 indicates $CaO/SiO_2 = 3.2$, Na_2O content = 15 mol.%.

Using these boundary definitions as guides, it is possible to identify several phase assemblages in the CaO-rich region of the diagram (Fig. 7) as follows:

1. $Ca(OH)_2$ + C-(A)-S-H: C-A-S-H composition ranges from $C_{1.94}SH_x$ to $C_{1.94}A_{0.06}SH_x$.
2. $Ca(OH)_2 + AF_m$ + C-A-S-H: The AF_m corresponds to the hemicarboaluminate and monocarboaluminate phases identified by XRD and the C-A-S-H composition is fixed at $C_{1.94}A_{0.06}SH_x$.
3. AF_m + C-A-S-H: C-A-S-H compositions in this field range from $C_{0.95}A_{0.06}SH_x$ to $C_{1.94}A_{0.06}SH_x$.

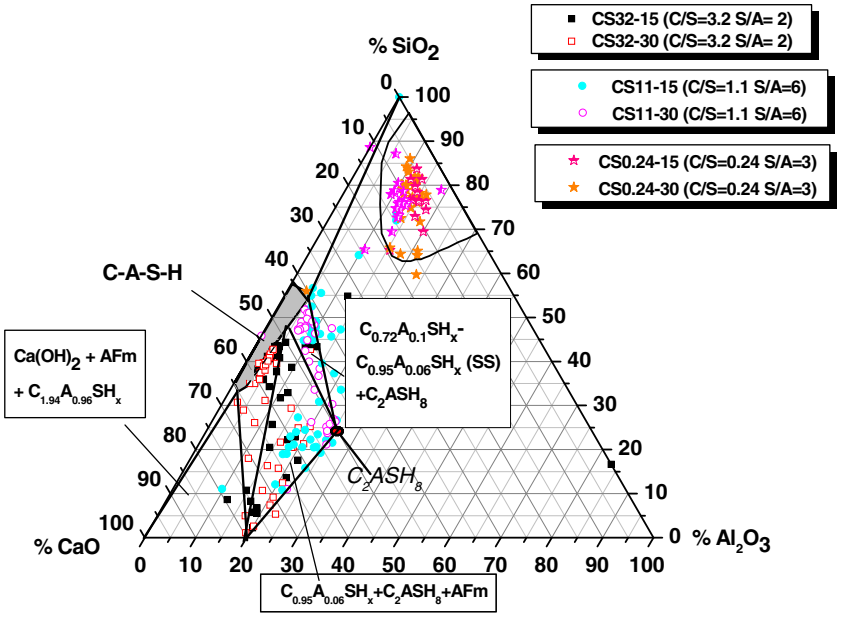

Fig. 7. $CaO–Al_2O_3–SiO_2–H_20$ projection diagram showing the tentative phase field boundaries proposed. Highlighted area indicates probable extent of C-A-S-H gels while the shaded region indicates the proposed compositional limits of a (C,N)-A-S-H gels. Original bulk aqueous compositions are indicated in the figure legend by the label format $CS(CaO/SiO_2)$–(mol.% Na_2O); e.g. CS32-15 indicates $CaO/SiO_2 = 3.2$, Na_2O content = 15 mol.%.

4. C-A-S-H + C_2ASH_8 + AF_m: C-A-S-H composition is fixed at $C_{0.95}A_{0.06}SH_x$
5. C-A-S-H + C_2ASH_8: C-A-S-H composition ranges from $C_{0.72}A_{0.1}SH_x$ to $C_{0.95}A_{0.06}SH_x$

It is interesting to note that tie lines drawn from the AFm and the C_2ASH_8 compositions respectively to $C_{0.95}A_{0.06}SH_x$ provide limits to different clusters of compositions observed in the present study. This adds some weight to the significance of the $C_{0.95}A_{0.06}SH_x$ composition as marking a shift in C-A-S-H characteristics.

It is not yet clear if strätlingite exhibits variation in composition in the direction of C-A-S-H or not but as stated above, the present analyses was unable to differentiate C_2ASH_8 from C-A-S-H in the region designated as 'C-A-S-H' in Fig. 6. Indeed, according the field boundaries extrapolated from the data of Pardal et al.[15], few of the compositions precipitated are of pure C-A-S-H gel. According to Fig. 7, crystalline co-precipitates would be predicted where this region overlaps with assemblages 3, 4 and 5 as defined above. It can be emphasised that the indicated compositions in these phases fields, particularly those positioned close to the proposed C-A-S-H boundaries, correspond to C-A-S-H as the predominant phase, which could easily occlude and obscure finely dispersed and nano-dimensional crystallites.

3.1.2. CaO-deficient gels

In the CaO-deficient region of the diagram, compositions assigned to (N,C)-A-S-H show a relatively narrow distribution which permit the identification of the compositional limits expressed again relative to the $CaO–Al_2O_3–SiO_2$ plane ($0<CaO/SiO_2<0.3$ and $0.08<Al_2O_3/SiO_2<0.5$. The Na_2O content cannot be reliably determined by EDX but using the lever rule, approximate compositions can be defined (see Fig. 8). Using the Al_2O_3:SiO_2 ratios at the N-A-S-H compositional limits, the theoretical Na_2O content of an N-A-S-H gel can be determined (Na^+ is required to balance framework charge). By intercepting the tie lines between the theoretical N-A-S-H composition and CaO and the tie line between Na_2O and the position projected on the $CaO–Al_2O_3–SiO_2$ plane arising from EDX analysis, the precise composition of the calcium modified N-A-S-H ((N,C)-A-S-H) can be defined. Correspondingly, compositional limits for the low lime compositions are $0<Na_2O/Al_2O_3<1.85$, $0<CaO/SiO_2<0.3$.

A further and perhaps more relevant expression of (N,C)-A-S-H composition may be to recognise the ion exchange properties of the framework N-A-S-H gel. As Ca^{2+} is known to displace Na^+ in ion exchanging substrates, e.g. clay minerals, zeolites, it is relevant to consider that the precipitated N-A-S-H, if stable, may support ion exchange. Based on the approach taken to fix (N,C)-A-S-H compositions above, the Ca loading can be expressed as a percentage of the ion exchange capacity (IEC) (see Table 2). It is significant that this approach shows that Ca has occupied between 67 and 100% of the available sites, i.e. suggesting that the N-A-S-H precipitated from these CaO-deficient preparations is stable and behaves as an ion exchanger. This behaviour is consistent with N-A-S-H being characterised in the literature as a zeolite-precursor.

Table 2
CaO content and IEC calculated for (N,C)-A-S-H gels.

	CaO content (mol.%)	IEC (equiv/100mols)	Ca as % of capacity
Low	14	42	67
High	7	14	100

IEC: Ion exchange capacity.

3.1.3. Effect of pH

The observed co-existence of (N,C)-A-S-H and C-A-S-H gels however remains unexplained when referenced against the compositional distributions in Fig. 7 which show a rather evident gap between the respective phase fields. In fact, pH measurements on equilibrated solutions reveal that for all high and medium calcium preparations, pH was in excess of 12.0. The corresponding data for precipitated N-A-S-H gels shows pHs between 9.5 and 12.0.

Given the clear relationship between N-A-S-H gels and zeolites, it is helpful to consider the wider experience of zeolites in cement systems. It is well known that zeolites are synthesised under high pH conditions (just as initiation of geopolymerisation requires high pH) and they are stable to high pH in certain conditions. However, it is also known that zeolites behave pozzolanically in cement systems [16], degrading to produce essentially C-A-S-H. It is therefore proposed that the stability of N-A-S-H can be represented in a pseudo phase diagram (Fig. 9) which shows that at cement relevant pHs and in the presence of Ca, N-A-S-H degrades to C-A-S-H. Initially, C-A-S-H of minimum Ca content would be precipitated but as Ca concentration increases and N-A-S-H is exhausted, the CaO/SiO_2 would increase as the composition moves through the C-A-S-H-containing phase fields towards CaO (Fig. 7). If the pH is low enough (<12), N-A-S-H persists, even in the presence of Ca, accepting Ca by an ion exchange mechanism to give (N,C)-A-S-H until all Na has been replaced by Ca (if sufficient Ca is available). Note that at low pH, a fully Ca-exchanged 'N'-A-S-H may appear to have a C-A-S-H composition, but in this case, it retains its 3D aluminosilicate framework structure and is easily distinguishable from a 2D C-A-S-H gel [2]. The role of Ca in complexing silicates/aluminosilicates is essentially driven by the strong polarising power of the aqueous Ca ion relative to the alkali metal ions Na^+(aq) and K^+(aq). This theme is developed more widely in a separate publication [17].

3.2. Direct mixing of gels

The foregoing discussion has focussed on experimental procedures designed to provide rapid equilibration. Observations in 'real' systems are sometimes given more emphasis in the literature but it is important to recognise that all systems will endeavour to approach

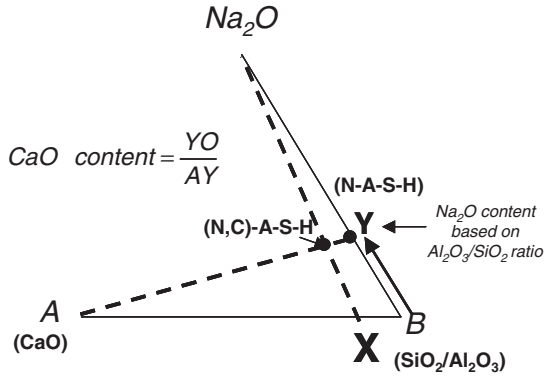

Fig. 8. Use of the Lever rule from the EDX data plotted in the $CaO–Al_2O_3–SiO_2–H_2O$ projection diagram.

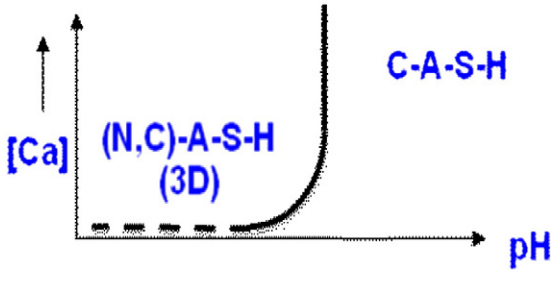

Fig. 9. Model proposed for the stability of N-A-S-H gel as a function of pH and Ca concentration. At low pH, Ca^{2+} association with the 3D aluminosilicate framework is by ion exchange with Na^+ up to saturation (broken line).

equilibrium if conditions allow, e.g. adequate reactants, access to reactive centres, etc. To address this, the direct mixing of gels enables an assessment of the relationship between the 'equilibrium' and 'real' datasets.

Fig. 10(a) and (b) shows respectively the evolution of N-A-S-H and C-S-H mixtures and N-A-S-H and C-A-S-H mixtures respectively. Fig. 10(a) shows the already well recognised substantial shift in position and shape of the νas Si–O absorption band when comparing C-S-H and N-A-S-H gels (at 960 cm^{-1} for C-S-H and at 1060 cm^{-1} for N-A-S-H) [12,14]. Of greater significance is the evolution of FTIR spectra with time after mixing. Using the main absorbancies for C-S-H (ν_{as} of Si–O–Si bonds) and for N-A-S-H gel (ν_{as} of T–O–T bonds where T is Si or Al around 1060 cm^{-1}[14]) it is possible to observe (i) a deepening of the absorbance associated with the C-S-H gel, the position of which remains fairly constant, and (ii) a broadening of the absorbance associated with the N-A-S-H gel. It is to be notice that the contribution of the band associated with C-S-H gel in these normalised spectra increases with time but even after 28 days, the spectra tend to suggest the coexistence of a 'N-A-S-H'-type structure and a 'C-A-S-H' type structure.

In the N-A-S-H + C-(A)-S-H mixtures (See Fig. 10(b)) the broader peak corresponding to N-A-S-H gels gradually diminishes with time leaving peaks predominantly of C-(A)-S-H character. This is an important indicator of the incompatibility of reactivity between these two gels.

To understand the significance of these observations, it is necessary to consider the starting compositions of both gel types, in each case, and in relation to the proposed phase diagram in Fig. 7. The situation is reproduced in Fig. 11 where Fig. 11(a) and (b) shows respectively the results of analyses by TEM/EDX for each of the gel mixtures; compositions for starting gels and for the mixtures after 28 days are indicated. However, following the publication by Pardal et al.[15], it can be noted that most of the synthetic 'C-A-S-H' products are likely to be phase mixtures containing C-A-S-H, as *bulk* compositions lie outside the shaded C-A-S-H field.

Fig. 11(a) shows that mixtures of pre-made C-S–H and N-A-S-H produce products of compositions defined by two distinct clusters, one indicative of C-A-S-H and the other within the area previously identified with (C,N)-A-S-H. (C,N)-A-S-H gels were not anticipated as products in this system as it was expected that pH would be buffered to >12. In this case, (C,N)-A-S-H would be expected to be unstable in the presence of Ca (see above). Nevertheless, the existence of the two compositional clusters confirms the characteristics of the FTIR spectra in Fig. 10 which indicate gels of both character being present. Either C-A-S-H only, or a mixture of C-A-S-H gel (in the compositional range $C_{0.72}A_{0.1}SH_x$ to $C_{0.95}A_{0.06}SH_x$) and N-A-S-H would be predicted at equilibrium, based on the proposed phase diagram (Fig. 7); a (C,N)-A-S-H gel would not be predicted unless pH had dropped. In fact, for this system, the pH at 28 days *had* dropped to 11.68, which would account for the existence of (C,N)-A-S-H.

Fig. 11(b) shows compositions which appear to indicate an enhanced degree of reactivity between the starting materials, based on the FTIR (Fig. 10) and EDX data. No obvious clustering in the (C,N)-A-S-H region is evident this time, presumably because in this system, the measured pH remained sufficiently high; i.e. in fact, measurements confirmed that pH in this mixture was 12 at 28 days.

Resulting compositions are distributed between starting gel compositions. No intermediate phases are anticipated between C-A-S-H (of minimum CaO/SiO_2 and maximum Al_2O_3/SiO_2 ratio) and N-A-S-H gels so, based on the proposed phase equilibria, it is suggested that the observed compositions represent intimate mixtures of N-A-S-H, C-A-S-H and possibly gehlenite hydrate. However, it is highly possible that these data do not yet represent an equilibrium system and that phase compositions are still evolving. This is probably the most likely situation given that existing precipitates, coming into contact in suspension, must go through a dissolution-reprecipitation process with associated diffusional implications impacting on overall reaction rate.

Further development of the phase diagram towards more Al_2O_3-rich compositions will be necessary to enable better reliability in predicting the relevant phase assemblages. Note that this study, and therefore the proposed equilibrium phase diagram including identified phase assemblages, is only relevant to 25 °C and 1 atmosphere (the experimental conditions) and is not necessarily compatible with

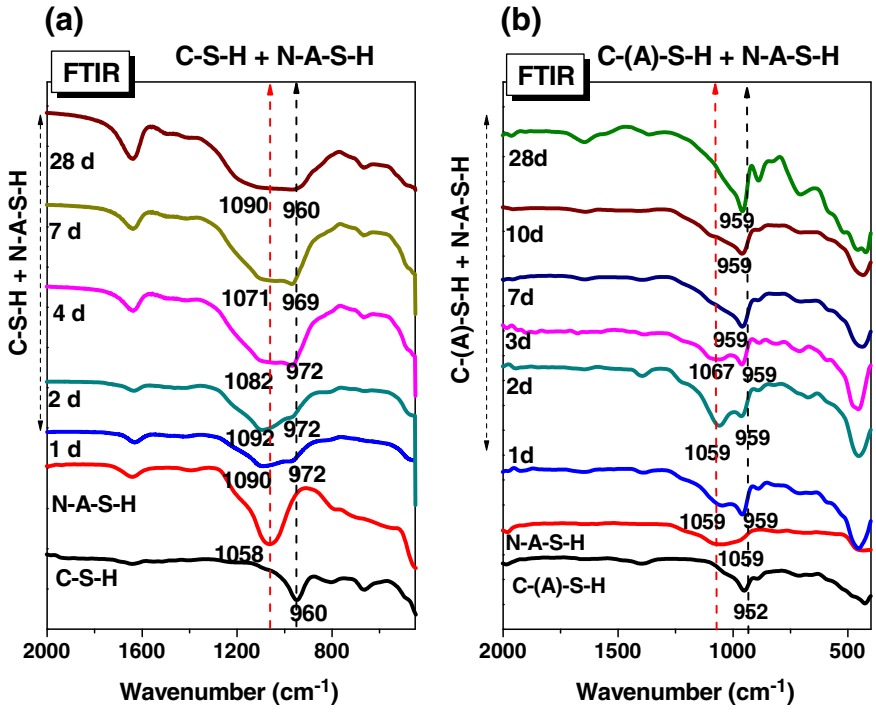

Fig. 10. FTIR spectra for mixtures of (a) C-S-H and N-A-S-H (b) C-(A)-S-H + N-A-S-H.

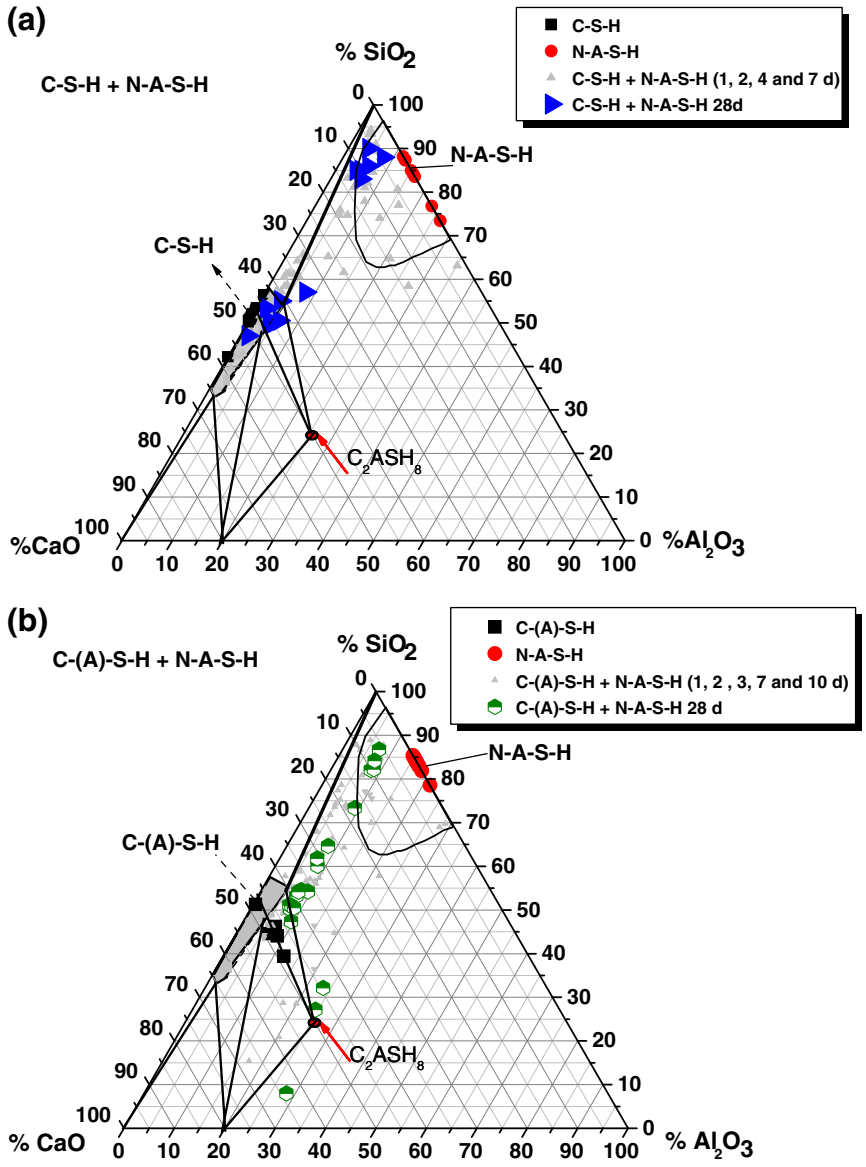

Fig. 11. $CaO–Al_2O_3–SiO_2–H_20$ projection diagram with the EDX analyses of gels arising from the direct mixing of gels (a) C-S-H + N-A-S-H (b) C-A-S-H + N-A-S-H.

diagrams of this system or portions of it derived from data obtained under other conditions, e.g. elevated temperature or pressure (e.g. hydrothermal syntheses).

4. Conclusions

Based on a series of solution/precipitation studies, a tentative phase diagram has been proposed for the Na_2O-CaO–Al_2O_3–SiO_2 system at 25 °C. At cement relevant pH, the dominating phase is a solid solution designated C-A-S-H having the compositional range $0.72<CaO/SiO_2<1.94$ and $0<Al_2O_3/SiO_2<0.1$; there is negligible Na_2O content in this and in related CaO-rich phases. Note that in the present study, all phases are assumed to be water saturated.

C-A-S-H is observed to be compatible with $Ca(OH)_2$, mono- and hemi-carboaluminates and strätlingite but the relationships in the lime-rich portion of the diagram are partitioned into 5 phase fields:

1. $Ca(OH)_2$ + C-(A)-S-H: C-A-S-H composition range from $C_{1.94}SH_x$ to $C_{1.94}A_{0.06}SH_x$.
2. $Ca(OH)_2 + AF_m$ + C-A-S-H: C-A-S-H composition is fixed at $C_{1.94}A_{0.06}SH_x$.
3. AF_m + C-A-S-H: C-A-S-H compositions range from $C_{0.95}A_{0.0.06}SH_x$ to $C_{1.94}A_{0.06}SH_x$.
4. C-A-S-H + C_2ASH_8 + AF_m: C-A-S-H composition is fixed at $C_{0.95}A_{0.06}SH_x$
5. C-A-S-H + C_2ASH_8: C-A-S-H composition ranges from $C_{0.72}A_{0.1}SH_x$ to $C_{0.95}A_{0.06}SH_x$

A three-dimensionally structured gel designated N-A-S-H is also observed in this system but in the presence of Ca, it is only stable at low pH (<12). This is the well known N-A-S-H gel from alkali-activation of aluminosilicate systems but the present study has shown that at high pH (>12), the presence of Ca will degrade N-A-S-H in favour of C-A-S-H formation. When stable at low pH, it behaves as a zeolite, and exhibits ion exchange; Ca displaces Na until available Ca is exhausted. The compositional range for Ca-modified (ion exchanged) (C,N)-A-S-H gels is $0<Na_2O/Al_2O_3<1.85$, $0<CaO/SiO_2<0.3$, $0.05<Al_2O_3/SiO_2<0.43$.

Direct mixing of pre-synthesised C-S-H or C-A-S-H gels with N-A-S-H leads to reactivity between the gels. It is expected that gradual degradation of N-A-S-H to C-A-S-H will occur until a C-A-S-H composition corresponding to its minimum CaO/SiO_2 and maximum

Al_2O_3/SiO_2 ratio is reached. Thereafter, an equilibrium mixture of the remaining N-A-S-H and C-A-S-H is predicted, based on the results of the precipitation/solubility studies.

Acknowledgement

The support of NANOCEM, a European industrial/academic partnership for fundamental research on cementitious materials, is acknowledged. Valuable discussions with Duncan Herfort, Thomas Matschei, Ellis Gartner and Karen Scrivener are also gratefully acknowledged.

References

[1] A. Palomo, M.W. Grutzeck, M.T. Blanco, Alkali-activated fly ashes—a cement for the future, Cem. Concr. Res. 29 (1999) 1323–1329.
[2] J.L Provis, J.S.J van Deventer, Geopolymers: Structures, Processing, Properties and Applications, Ed. Woodhead Publishing Limited, University of Melbourne, Australia, (2009).
[3] P. Duxon, A. Fernández-Jiménez, J.L. Provis, G.C. Lukey, A. Palomo, J.S.J. van Deventer, Geopolymer technology: the current state of the art, J. Mater. Sci. 42 (2007) 2917–2933.
[4] D. Khale, R. Chaudhary, Mechanism of geopolymerization and factors influencing its development: a review, J. Mater. Sci. 42 (2007) 729–746.
[5] C.K. Yip, G.C. Lukey, J.S.J. van Deventer, The coexistence of geopolymeric gel and calcium silicate hydrate at the early stage of alkaline activation, Cem. Concr. Res. 35 (2005) 1683–1697.
[6] A. Palomo, A. Fernández-Jiménez, G. Kovalchuk, L.M. Ordoñez, M.C. Naranjo, Opc-fly ash cementitious systems: study of gel binders produced during alkaline hydration, J. Mater. Sci. 42 (2007) 2958–2966.
[7] I. García-Lodeiro, D.E. Macphee, A. Palomo, A. Fernández-Jiménez, Effect of alkalis on fresh C-S-H gels. FTIR analysis, Cem Concr. Res. 39 (2009) 147–153.
[8] I. García-Lodeiro, A. Fernández-Jiménez, A. Palomo, D.E. Macphee, Effect on fresh C-S-H gels of the simultaneous addition of alkali and aluminium, Cem. Concr. Res. 40 (2010) 27–32.
[9] I. Garcia-Lodeiro, A. Fernández-Jiménez, D. Macphee, A. Palomo, Effects of calcium addition on N-A-S-H cementitious gels, J. Am. Ceram. Soc. (2010) 1–7.
[10] I. Garcia-Lodeiro, D.E. Macphee, A. Fernández-Jiménez, A. Palomo, Compatibility studies between N-A-S-H and C-A-S-H gels. Study in the ternary diagram Na_2O-CaO-Al_2O_3-SiO_2-H_2O. Proceedings 13th International Congress on the Chemistry of Cement, July 2011, Madrid, Spain.
[11] F. Cassagnabére, M. Mouret, G. Escadeillas, Early hydration of clinker–slag–metakaolin combination in steam curing conditions, relation with mechanical properties, Cem. Concr. Res. 39 (2009) 1164–1173.
[12] Ping Yu, R.J. Kirkpatrick, B. Poe, P.F. McMillan, X. Cong, Structure of calcium silicate hydrate (C-S-H): near-, mid-, and far-infrared spectroscopy, J. Am. Ceram. Soc. 82 (3) (1999) 742–748.
[13] I. García-Lodeiro, A. Fernández-Jiménez, M. Teresa Blanco, A. Palomo, FTIR study of the sol–gel synthesis of cementitious gels: C-S-H and N-A-S-H, J. Sol-Gel Sci. Technol 45 (2008) 63–72.
[14] A. Fernandez Jimenez, A. Palomo, Alkali activated fly ashes. Structural studies through mid-infrared spectroscopy, Micropor. Mesopor. Mater. 86 (2005) 207–214.
[15] X. Pardal, I. Pochard, A. Nonat, Experimental study of Si–Al substitution in calcium-silicate-hydrate (C-S-H) prepared under equilibrium conditions, Cem. Concr. Res. 39 (2009) 637–664.
[16] F.P. Glasser, K. Luke, M.J. Angus, Modification of cement pore fluid compositions by pozzolanic additives, Cem. Concr. Res. 18 (1988) 165–178.
[17] D.E Macphee, I. Garcia-Lodeiro, Activation of aluminosilicates-some chemical considerations, Proceedings of the Second International Slag Valorisation Symposium. The Transition to sustainable Materials Management, 18-20 April , Leuven, Belgium (2011) 51-61.